

# Improvement of Spatial Resolution of Breast Cancer Detection Using 4x4 UWB Antenna Array with Impedance Matching Layer

T. Sugitani<sup>\*1</sup>, S. Kubota<sup>1</sup>, L. Xu<sup>2</sup>, X. Xiao<sup>2</sup> and T. Kikkawa<sup>1</sup>

<sup>1</sup> Research Institute for Nanodevice and Bio Systems, Hiroshima University  
1-4-2 Kagamiyama, Higashi-hiroshima, Hiroshima 739-8527, Japan.

Phone: +81-82-424-7879, Fax: +81-82-424-3499, E-mail: {sugitani-takumi2, kikkawat}@hiroshima-u.ac.jp

<sup>2</sup> School of Electronic and Information Engineering, Tianjin University, Tianjin 300072, China

**Abstract**— A 4x4 planar ultra-wideband (UWB) antenna array with a matching layer to breast skin and fat was developed for radar-based breast cancer detection system. The antenna array with the matching layer with a thickness of 0.25 mm and dielectric constant of 2.0 could improve the spatial resolution of two separate 5-mm-diameter spherical tumor phantoms, which were located at the depth of 22 mm with the spacing of 8 mm.

## 1. Introduction

X-Ray mammography is currently the most common technique used in breast cancer screening. It employs ionizing radiation and requires uncomfortable compression of the breast during the examination. These limitations of mammography have resulted in research into alternative methods for imaging breast cancer. It has been reported that the permittivity and conductivity of breast cancer tissues were higher than that of normal breast tissue [1] so that radar-based breast cancer detection systems using ultra-wide-band (UWB) signals have been developed. UWB technologies have been applied to short range communication technology which transmits and receives the signals in the form of very short pulses such as Gaussian monocycle pulses (GMP) [2, 3]. In order to develop a handheld screening system, we have proposed a compact mobile system in the supine position for breast cancer detection [4-8], in which generation and transmission of GMP signals have been achieved by complementary metal oxide semiconductor integrated circuits (CMOS-IC) [9, 10].

In this paper, the confocal imaging technique using UWB antenna array was developed and the effects of matching layer and UWB antenna array configuration on the spatial resolution of breast cancer detection were investigated.

## 2. Effect of Matching Layer and Array Configuration

The center frequency of the transmitted Gaussian monocycle pulse was 6 GHz. The antenna consists of a square slot in a ground plane on one side of a Duroid RT 6010LM substrate with a relative permittivity of 10.2. Figure 1 shows the schematic cross-section of a breast phantom structure. Figures 2(a) and 2(b) show the simulation results of reflection coefficient ( $S_{11}$ ) and transmission coefficient ( $S_{21}$ ) versus frequency as a parameter of the permittivity of the matching layer. The optimum dielectric constant  $\epsilon_{\text{matching layer}}$  of 2 was chosen,

which had the largest bandwidth. Figures 3(a) and 3(b) show the simulation results of  $S_{11}$  and  $S_{21}$  versus frequency as a parameter of matching layer thickness. The thickness  $t$  of 0.25 mm was chosen, which had the largest bandwidth. Figure 4 shows the antenna transmission gain of the antenna with and without matching layer as a function of frequency. The antenna transmission gain increased +5.4 dB at 6 GHz with the matching layer.

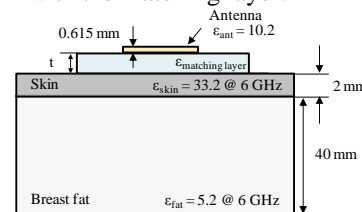


Fig. 1. Schematic cross-section of breast phantom structure.

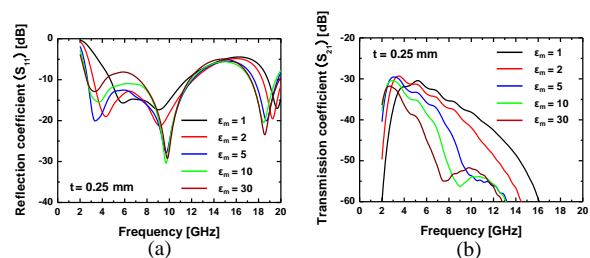


Fig. 2. Influence of permittivity of the matching layer on S-parameters. (a) Reflection coefficient ( $S_{11}$ ) versus frequency. (b) Transmission coefficient ( $S_{21}$ ) versus frequency.

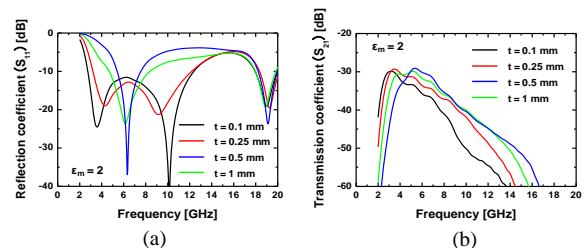


Fig. 3. Influence of the thicknesses of the matching layer. (a)  $S_{11}$  versus frequency. (b)  $S_{21}$  versus frequency.

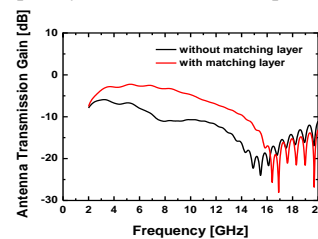


Fig. 4. Calculated antenna gains with and without matching layer as a function of the frequency.

Figures 5(a), 5(b) and 5(c) show the antenna array configuration, in which isolation and aperture size were changed. 5-mm-diameter spherical tumor phantoms with a relative permittivity of 47 at 6 GHz were embedded at the depth of 22 mm. Figure 6 shows frequency spectra of subtracted waveforms of received GMP with and without tumor phantoms. The amplitude of the tumor response was improved approximately twice by use of matching layer.

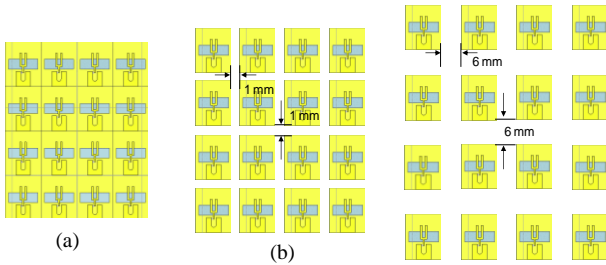


Fig. 5. Antenna array configuration. (a) No isolation. (b) 1 mm isolation slit. (c) 6 mm isolation slit.

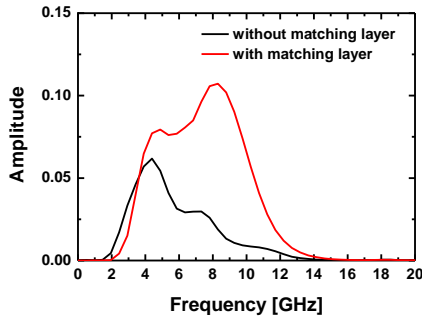


Fig. 6. Effect of matching layer on frequency spectra of Gaussian monocycle pulse subtracted waveform.

Figures 7(a), 7(b), 7(c), 7(d), 7(e), and 7(f) show spatial resolution of confocal imaging of 5-mm-diameter spherical tumor phantoms with the separation distance of 8 mm. Two separate breast tumors with the separation distance of 8 mm were resolved by use of 6 mm isolation slit and the energy of the tumor response was five times greater by use matching layer as shown in Figs. 7(g) and 7(h).

### 3. Conclusions

Effects of matching layer and isolation of 4x4 planar antenna arrays on the bandwidth and gain of the antenna were investigated for breast cancer detection. Antenna transmission gain was improved +5.4 dB at 6 GHz by use of the matching layer with a thickness of 0.25 mm and the dielectric constant of 2.0. Two separate breast tumor phantoms having the 5-mm-diameter spherical tumors with the separation distance of 8 mm were resolved by use of 6 mm isolation slit antenna array with the matching layer.

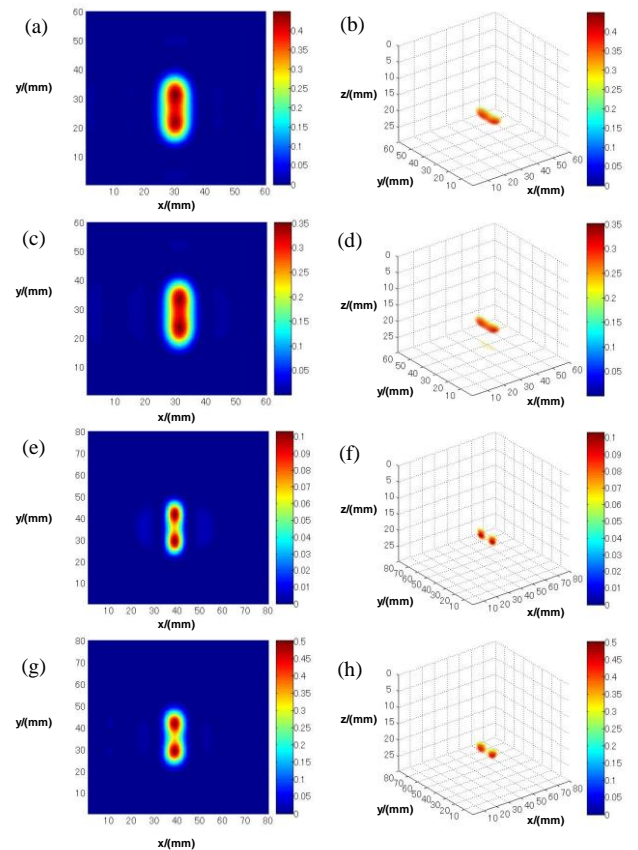


Fig. 7. Spatial resolution of confocal images of 5-mm-diameter spherical tumor phantoms with the separation distance of 8 mm. (a) 2D image without array isolation. (b) 3D image without array isolation. (c) 2D image with 1 mm isolation slit. (d) 3D image with 1 mm isolation slit. (e) 2D image with 6 mm isolation slit. (f) 3D image with 6 mm isolation slit. (g) 2D image with both 6 mm isolation slit and matching layer. (h) 3D image with both 6 mm isolation slit and matching layer.

### References

- [1] X. Li, and S. C. Hagness, *IEEE Microwave Wireless Components Lett.*, vol. 11, pp. 130-132, 2001.
- [2] T. Kikkawa, P. K. Saha, N. Sasaki, and K. Kimoto, *IEEE J. Solid-State Circuits*, Vol. 43, No. 5, pp.1303-1312, May 2008.
- [3] N. Sasaki, K. Kimoto, W. Moriyama, and T. Kikkawa, *IEEE J. Solid-State Circuits*, Vol. 44, No. 2, pp.382-393, February 2009.
- [4] X. Xiao and T. Kikkawa, *Japanese Journal of Applied Physics* Vol. 47, No. 4, pp. 3209–3213, 2008.
- [5] S. Kubota, Xia Xiao, N. Sasaki, Y. Kayaba, K. Kimoto, W. Moriyama, T. Kozaki, M. Hanada and T. Kikkawa, *Japanese Journal of Applied Physics*, Vol.49, pp. 097001-1 – 097001-6, 2010.
- [6] T. Sugitani, et al., *IEEE International Symposium on Antennas and Propagation and UNSC/URSI National Radio Science Meeting*, 356. 10. Chicago, USA, July 8-14, 2012.
- [7] T. Sugitani, et al., *International Conference on Solid State Devices and Materials*, PS-11-1, Kyoto, September 25-27, 2012
- [8] T. Sugitani, et al., *International Symposium on Electromagnetic Theory*, 23AM1B07, Hiroshima, May 20-24, 2013
- [9] A. Toya, N. Sasaki, S. Kubota and T. Kikkawa, *Japanese Journal of Applied Physics*, Vol. 50, No. 4, pp. 04DE02-1 – 7, Apr. 2011.
- [10] M. Hafiz, S. Kubota, N. Sasaki, K. Kimoto and T. Kikkawa, *IEICE Transactions on Electronics* Vol. 94-C, No. 6, pp. 977 – 984, Jun. 2011.